Contour-Based Structure from Reflection

Po-Hao Huang Shang-Hon Lai
Department of Computer Science, National Tsing Hua University, Hsinchu, Taiwan
{even, lai}@cs.nthu.edu.tw

Abstract

In this paper, we propose a novel contour-based algorithm for 3D object reconstruction from a single uncalibrated image acquired under the setting of two plane mirrors. With the epipolar geometry recovered from the image and the properties of mirror reflection, metric reconstruction of an arbitrary rigid object is accomplished without knowing the camera parameters and the mirror poses. For this mirror setup, the epipoles can be estimated from the correspondences between the object and its reflection, which can be established automatically from the tangent lines of their contours. By using the property of mirror reflection as well as the relationship between the mirror plane normal with the epipole and camera intrinsic, we can estimate the camera intrinsic, plane normals and the orientation of virtual cameras. The positions of the virtual cameras are determined by minimizing the distance between the object contours and the projected visual cone for a reference view. After the camera parameters are determined, the 3D object model is constructed via the image-based visual hulls (IBVH) technique. The 3D model can be refined by integrating the multiple models reconstructed from different views. The main advantage of the proposed contour-based Structure from Reflection (SfR) algorithm is that it can achieve metric reconstruction from an uncalibrated image without feature point correspondences. Experimental results on synthetic and real images are presented to show its performance.

1. Introduction

The 3D reconstruction problem has been studied in computer vision for decades. Most of the 3D reconstruction algorithms require some feature point correspondences across views, which are usually obtained by either manual selection or automatic feature detection and matching algorithms. However, it is difficult to achieve very reliable feature correspondences, especially for the case with wide baseline. In addition, there is usually lack of feature correspondence in homogenous region. The contour-based approach integrates the object contour information from different view points for 3D object reconstruction without requiring feature correspondences. Many contour-based reconstruction algorithms have been proposed and they are often referred as SfS, SfC [8][9] or IBVH [4]. The contour-based approach does not require feature correspondences, but the camera information needs to be known or estimated before the 3D reconstruction.

In the proposed contour-based method, we can recover the 3D model of an object from a single image by placing it in front of two plane mirrors, as shown in Figure 1. Under this setting, several additional views of an object could be generated by mirror reflections in a single image. Hence, 3D reconstruction via IBVH from only one such image containing multiple mirror reflections is possible. This is principally equivalent to 3D reconstruction from multiple images at different views. However, we need to know exactly the camera information and the poses of mirrors to compute the poses of different viewpoints.

Figure 1. An example of the mirror image setting

The idea to generate novel view with plane mirror and recover the 3D structure had been proposed since early 80' and many related researches have been published till now. Previous methods in this approach either need to know the camera information or the poses of mirrors, or assume simplified camera projection models, such as affine transformation or orthographic projection.

0-7695-2646-2/06 $20.00 (c) 2006 IEEE

Mitsumoto et al. [1] introduced the concept of using vanishing point (VP) to reconstruct 3D shape without knowing the position of mirror, where the VP is decided automatically according to the voting of correspondences determined from line intersections. However, this method is only suitable for polyhedral objects and needs the camera intrinsic parameters to be known in advance. Zhang and Tsui [2] extended the problem of recovering 3D shape from bilateral symmetric objects [3][5] to arbitrary one by using mirror to construct the bilateral symmetric relation. In their work, both camera information and mirror position are known in prior and correspondences are manually selected. Huynh [6] proposed an algorithm to reconstruct 3D object models up to an affine transformation relative to an arbitrary affine coordinated frame defined by manually selected four coplanar world points whose orthogonal projections onto the mirror plane form a rectangle or parallelogram. Due to the assumption of affine camera model, the camera self-calibration is greatly simplified especially with manually selected correspondences. Forbes et al. [7] used two plane mirrors to generate five views for IBVH to recover 3D structure. They adopted the orthographic projection model under the assumption that the variations in depth for each silhouette in 3D are small with respect to the distance from camera. Under the simplified orthographic projection model, the camera intrinsic information is no longer required, and the remaining problem is to estimate the relative orientations and the translations.

In this paper, we develop a self-calibration algorithm by using the property of mirror reflection for 3D reconstruction under the setting of two plane mirrors. The minimal set of point correspondences required in the self-calibration are found automatically by finding the tangent lines between the object contours in the original image and its reflection. Unlike most of the previous methods, the proposed algorithm automatically estimates the camera parameters as well as the poses of mirrors with the perspective projection model, thus it can achieve metric reconstruction with self-calibration.

Very recently, Forbes et al. [10] proposed a solution to the same problem as ours by using the distances among epipoles and the geometrical similarities to derive a closed-form solution of focal length and principle point. In their work, the camera position is computed based on the epipolar tangency constraint and the focal length is derived from the geometrical similarities, which will be shown to be problematic under some situation in section 6. Note that our proposed solution is different from theirs [10] and it was developed independently of the recent work by Forbes el al. [10].

The remaining of this paper is organized as follows. Section 2 describes the geometry formed by a single plane mirror. Section 3 extends the relation to two plane mirrors and describes the self-calibration method. The procedure for determining the orientations and translations of the mirror planes is presented in section 4. Section 5 discusses how to integrate the IBVH reconstructed models obtained from different camera views of the object. Experimental results of both synthetic and real data are given in section 6. Finally, we conclude this paper in section 7.

2. The Geometry via Plane Mirror

Mirror reflects lights, thus we can see the other side of an object from the same viewing angle. The corresponding geometry established by placing a plane mirror in the scene can be illustrated in Figure 2. In the figure, Π_m is the mirror plane with plane normal n, X is an object point and its reflection X' could be imagined as a virtual point at the opposite side of the mirror plane, and C represents the camera center and the relative image plane is denoted by Π_i. In the same way, there exists a virtual camera on the other side of mirror and its associated virtual image plane Π_i'. Thus, the two view geometry for camera with a plane mirror is established.

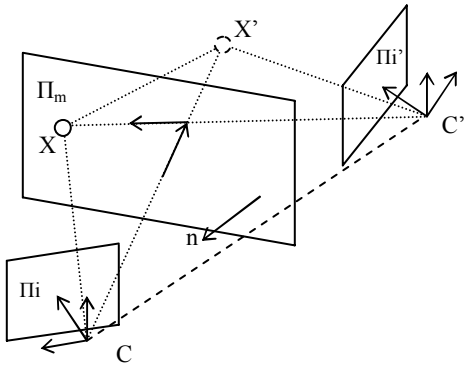

Figure 2. The geometry of a camera with a plane mirror.

2.1. Virtual Camera and Image

Because of mirror reflection, the virtual camera C' has left-handed coordinate system, and the virtual image viewed by virtual camera C' is identical to the image viewed by the camera C [5]. The projection of X' onto Π_i is to the same as the projection of X onto Π_i'. This property implies that one image containing a mirror reflection can be considered as two images from different viewing angles, thus 3D reconstruction is possible if we know the camera parameters.

2.2. The Epipolar Geometry

The epipole of Π_i is the projection of virtual camera center C', and the epipolar line corresponding to point X is the projection of $\overline{XC'}$.

In this particular system, the 3D line $\overline{XX'}$, which passes through any point X and its reflection X', is parallel to plane normal n and is perpendicular to the mirror plane. This brings an important property that the line joining the projection of X and X' onto Π_i will be the epipolar line [6][7], and the epipole is located at the intersection of these epipolar lines.

This property could be easily proved. Because the line $\overline{CC'}$ is also perpendicular to the plane normal n, we have $\overline{XX'} // \overline{CC'}$. Hence, points X, X', C, and C' are coplanar. The projection of $\overline{XX'}$ will be located on the same line as the projection of $\overline{XC'}$, i.e. the epipolar line.

2.3. Vanishing Point

Similar concept with respect to the previous section is the vanishing point. Recall that line $\overline{XX'}$, joining any point and its reflection, parallels to plane normal n. Thus, these parallel lines will intersect at plane infinity. After perspective projection, these projected lines will intersect at one point, the vanishing point (VP), denoted by e_∞ [1][7].

These two concepts tells us that e_∞ could be found by the intersection of lines joining the image corresponding points, and the plane normal n will be the inverse direction from camera center C to the VP e_∞.

2.4. Tangent Line

In this section, we will introduce the important concept that makes the automatic correspondence of a minimal point set possible, which is required in the self-calibration procedure. This property is also mentioned in [7].

As shown in Figure 3, assume that there is a plane Π_t passing through camera center C and virtual camera center C'. Its projection onto the image plane Π_i is line l_t and it will pass through the VP e_∞.

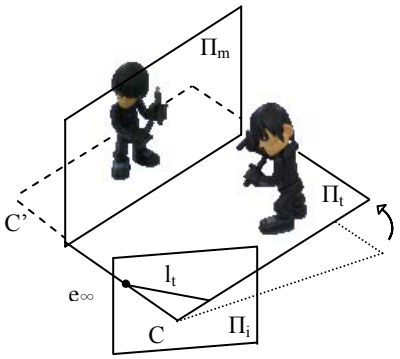

Figure 3. Tangent plane and the tangent line

There are two properties in this situation; namely, (i) line l_t is tangent to the object contour in image iff the tangent plane Π_t is tangent to some object point and (ii) if Π_t is tangent to some object point X, it must be tangent to the corresponding virtual point X' concurrently.

The property (i) can be justified as follows. Because l_t is the projection of plane Π_t, this plane only touches the object point X whose projection is x if l_t is tangent to the object contour at point x. Hence, plane Π_t is tangent to the object at X. On the other hand, if plane Π_t is tangent to some object point X, the projection line l_t will only pass through the projection of X. Therefore, the line l_t will be tangent to the object contour. We can justify property (ii) because X, X', C and C' are coplanar.

Thus, we can conclude that some epipolar lines will be tangent to both object contours simultaneously, and the joined tangent points form a correspondence pair of an object point and its reflection. This property gives us a way to find the correspondence automatically by finding the tangent lines of both object contours.

Figure 4 depicts an example of two contours and their tangent lines, two outers and two crosses. The outer lines are the epipolar lines, and the cross lines are not. Because the line tangent to object contour must intersect at the apex of the contour, we can firstly construct the convex hull for each contour. Because the epipolar line is the outer tangent line and it must concurrently be tangent to both contours, we can find the outer tangent lines by merging two convex hulls into one. The two line segments in the merged convex hull, which are determined by joining two points belonging to different contours, are the epipolar lines.

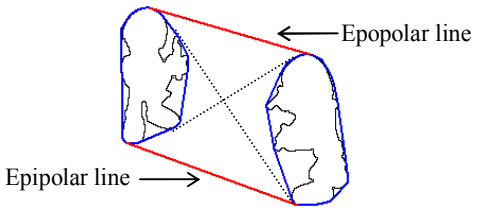

Figure 4. Tangent lines of two convex hulls

Therefore, we obtain an additional property that a pair of corresponding contours only has two tangent lines that are epipolar lines and these two tangent lines intersect at the VP e_∞, as mentioned in section 2.3.

3. Self-Calibration using Two Mirrors

A single mirror can only generate one additional viewing angle, and the number of correspondences is not enough for self-calibration. If there are two mirrors in the scene, we can obtain more views from the inter-reflections between two mirrors.

In this section, we focus on the case of five images (one real and four reflections) generated by two mirrors and give an algorithm for determining the camera intrinsic.

Here, we assume the calibration matrix has the simplified form with the only unknown – focal length

$$K = \begin{bmatrix} f & & c_u \\ & f & c_v \\ & & 1 \end{bmatrix} \quad (1)$$

where f is the focal length, and (c_u, c_v) is the principle point.

Under the assumption of zero skew, unit aspect ratio and principle point at the image center, the focal length f can be computed by solving a quadratic equation, and this simplification provides a good and practical approximation to the perspective camera projection model.

3.1. One Real and Four Reflections

For ease of explanation, we index the five views from obj_0 to obj_4 as shown in Figure 5.

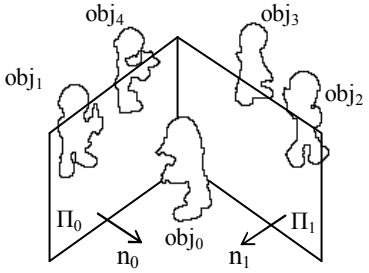

Figure 5. 5 views generated by two mirrors

Note that obj_0 is the real image, obj_1 and obj_2 are its reflections via Π_0 with normal n_0 and Π_1 with normal n_1, respectively, obj_3 is the reflection of obj_1 via Π_1, and obj_4 is the reflection of obj_2 via Π_0. The geometrical arrangement of these five views is more clearly illustrated from the bird's eye view as shown in Figure 6.

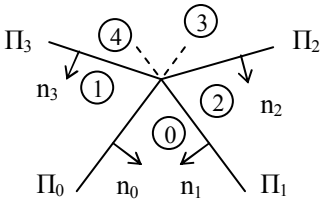

Figure 6. The bird's eye view of the mirror setting

Note that Π_2 is a virtual mirror plane of Π_0 according to mirror plane Π_1, thus the plane normal n_2, using the property of mirror reflection, can be express as

$$n_2 = n_0 - 2(n_0 \cdot n_1)n_1 \quad (2)$$

In the same manner, n_3 can be express as

$$n_3 = n_1 - 2(n_1 \cdot n_0)n_0 \quad (3)$$

3.2. Determining the Focal Length

From section 2, if we have a epipole $e_\infty = (e_x, e_y, 1)^T$, the corresponding plane normal can be written as

$$n = -\frac{(\hat{e}_x, \hat{e}_y, f)^T}{\|(\hat{e}_x, \hat{e}_y, f)\|} \quad (4)$$

where $\hat{e}_x = e_x - c_u, \hat{e}_y = e_y - c_v$, and the pixel per unit transformation factor is eliminated from normalization.

In the five views case, four vanishing points corresponding to four plane mirrors can be computed by locating the intersection of their corresponding tangent lines. Let e_0 to e_3 express the vanishing points for Π_0 to Π_3, respectively, and then we have

$$\begin{aligned} e_0 &= (e_{x0}, e_{y0}, 1)^T = \otimes(T_{01}, T_{24}) \\ e_1 &= (e_{x1}, e_{y1}, 1)^T = \otimes(T_{02}, T_{13}) \\ e_2 &= (e_{x2}, e_{y2}, 1)^T = \otimes T_{23} \\ e_3 &= (e_{x3}, e_{y3}, 1)^T = \otimes T_{14} \end{aligned} \quad (5)$$

where T_{ab} define the tangent lines between obj_a and obj_b and symbol "$\otimes$" expresses the intersectional operator.

Thus, the only and common unknown of each plane normal expression is the focal length.

From the reflection relationship, we can derive the following equations:

$$(n_0 + n_2) \cdot n_1 = 0 \quad (6)$$

$$(n_1 + n_3) \cdot n_0 = 0 \quad (7)$$

They can be easily verified by substituting eq. (2) and (3) into eq. (6) and (7), respectively.

The focal length can be determined by using equation (6) and (7) as follows. We first expand equation (6) and (7) with the parameterized form for the normal in equation (4) to obtain the following two equations.

$$f_1(\alpha) = \frac{v_{01} + \alpha}{\sqrt{v_{00} + \alpha}} + \frac{v_{21} + \alpha}{\sqrt{v_{22} + \alpha}} = 0 \quad (8)$$

$$f_2(\alpha) = \frac{v_{10} + \alpha}{\sqrt{v_{11} + \alpha}} + \frac{v_{30} + \alpha}{\sqrt{v_{33} + \alpha}} = 0 \quad (9)$$

where $v_{ab} = \hat{e}_{xa}\hat{e}_{xb} + \hat{e}_{ya}\hat{e}_{yb}$ and $\alpha = f^2$

Hence, we can solve f from the above two equations of the quadratic polynomial functions of α independently. To combine the above two constraints for determining the camera intrinsic that best fits the eqautions, we formulate this parameter estimation problem in a least-square framework and minimize the following cost function,

$$F(f) = f_1(f^2)^2 + f_2(f^2)^2 \quad (10)$$

After determining the focal length, each plane normal can be computed by using equation (4).

3.3. Co-linear Epipoles

Note that the vanishing points e_0 to e_3 are the projections of the virtual camera centers. These points should be co-linear, because all the camera centers are co-planar. Thus, we can make use of this property after calculating the epipoles by line fitting or using the two more reliable epipoles, e_0 and e_1, to decide the line that joins all the epipoles.

4. Camera Pose Estimation

After obtaining the camera intrinsic, the next step is to determine the camera extrinsic. To simplify the derivation, we assume the world coordinate system coincides with the real camera coordinate system, i.e.

$$R_0 = I_{3\times3} \text{ and } t_0 = 0_{3\times1} \tag{11}$$

In the following, we describe how we determine the poses for all the virtual cameras.

4.1. Orientation Determination

Having computed the plane normals, we can calculate the relative orientations of the virtual cameras by using the property of mirror reflection. Thus, we have the following equations

$$\begin{aligned} R_1 &= R_0 - 2R_0 n_0 n_0^T \\ R_2 &= R_0 - 2R_0 n_1 n_1^T \\ R_3 &= R_1 - 2R_1 n_1 n_1^T \\ R_4 &= R_2 - 2R_2 n_0 n_0^T \end{aligned} \tag{12}$$

Notice that, R_0, R_3 and R_4 belong to the right-handed coordinate system, while R_1 and R_2 belong to the left-handed coordinate system. For computational convenience, we do not make these coordinate systems consistent. The details will describe in section 4.4.

4.2. Translation Determination

Figure 7 depicts the spatial relationship of the real and virtual cameras with the two plane mirrors. Assume v_i denote the unit vector from C_0 to X_i, and then we can express X_i as

$$X_i = \lambda_i v_i \tag{13}$$

where λ_i is the distance from X_i to C_0. Because $\overline{X_1 X_{2_i}} \,//\, n_0$, we can derive the following relationship

$$(\lambda_1 v_1 - \lambda_2 v_2) \times n_0 = 0 \tag{14}$$

Hence, we have

$$\lambda_2 = (v_1 \times n_0) \cdot (v_2 \times n_0) / \|v_2 \times n_0\|^2 \lambda_1 = \alpha\lambda_1 \tag{15}$$

$$t_1 = \lambda_1 (\alpha v_2 + v_1 - 2(v_1 \cdot n_0) \cdot n_0) \tag{16}$$

Equation (16) means that translation vector t_1 can be determined up to an unknown scale λ_1 and the scale factor depends on how large the object is.

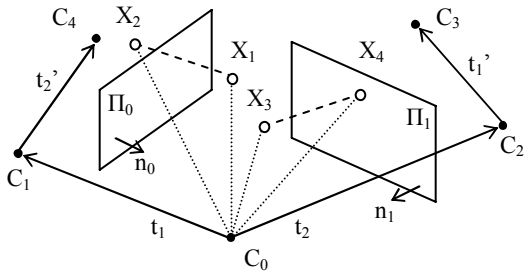

Figure 7. Spatial relationship for all the real and virtual cameras with the two plane mirrors

Similarly, the translation vector t_2 is also up to a different unknown scale. Thus, we have

$$\lambda_4 = (v_3 \times n_1) \cdot (v_4 \times n_1) / \|v_4 \times n_1\|^2 \lambda_3 = \beta\lambda_3 \tag{17}$$

$$t_2 = \lambda_3 (\beta v_4 + v_3 - 2(v_3 \cdot n_1) \cdot n_1) \tag{18}$$

If we know the ratio between λ_1 and λ_3, the translation vectors can be determined consistently, but it requires some spatial information about the object.

An alternative way is to assume point X_1 equal to X_3, and it means that we have to find a point in obj_0 and its reflections in obj_1 and obj_2 from the image. We can easily identify a pair of point correspondence via the tangent line between two objects (ex. obj_0 and obj_1) for some object point, but it is not straightforward to find the corresponding point in obj_2 of the same object point.

However, the correspondence point in obj_2 must lie on the line from the point in obj_1 to the epipole located by the tangent lines of obj_0 and obj_2, as shown in Figure 8. Thus, the possible region for the correspondence point is the red line enclosed by the contour of obj_2.

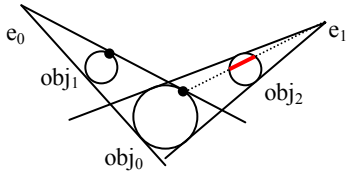

Figure 8: Finding the correspondence points in three views.

To find the correct position of the corresponding point in the third view, we define an error measurement function to evaluate each point that lies within the bounded line segment. The point with the minimal function value is regarded as the point of correspondence.

After obtaining the correspondence point, the translation vectors t_1 and t_2 can be computed via equation (16) and (18),

respectively. Additionally, the translation vectors t_3 and t_4 can be computed as

$$t_3 = t_2 + t_1' = t_2 + (t_1 - 2(t_1 \cdot n_1)n_1) \quad (19)$$

$$t_4 = t_1 + t_2' = t_1 + (t_2 - 2(t_2 \cdot n_0)n_0) \quad (20)$$

where t_1' is the reflection of t_1 via mirror plane Π_1 and t_2' is the reflection of t_2 via mirror plane Π_0.

The common scalar factor λ_1 (= λ_3) can be arbitrarily given, because we don't known exactly the object size. Thus, it's a metric reconstruction (Euclidean reconstruction up to an unknown scale).

4.3. Distance Minimization

If the camera parameters for each view are correct, the projection of visual cone generated by each of the other views should be tangent to and covers the object contour, as shown in Figure 9.

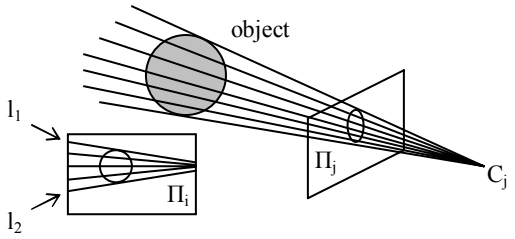

Figure 9. Visual cone and its projection onto other view

Thus, to find the correct correspondence point in obj_2 as described in section 4.3, we can generate a visual cone from virtual camera 1 and then project the visual cone to other cameras to evaluate if the visual cone is tangent to and covers all the object contours.

The error measurement function is defined as

$$F(x) = \sum_{i=0}^{i=4} \sum_{c_i \in CH_i} p(c_i, l_{1i}, l_{2i}) \quad (21)$$

where x is the candidate point on the bounded line segment in obj_2, CH_i is the convex hull of the object contour on image i and c_i's are the points that define the convex hull CH_i. Note that l_{1i} and l_{2i} are the two most outer lines of the projected visual cone on image i as shown in Figure 9, and p( ) is the penalty function defined by

$$p(c, l_1, l_2) = \begin{cases} 0 & , c^T l_1 c^T l_2 \le 0 \\ \min(d(c, l_1), d(c, l_2)) & , c^T l_1 c^T l_2 > 0 \end{cases} \quad (22)$$

where d( ) is the function evaluating the distance from point c to line l.

Note that $c^T l_1 c^T l_2$ is negative if point c lies between line l_1 and l_2, it is zero if point c lies on line l_1 or l_2, and it is positive otherwise.

Actually, we only need to project the virtual cone of one view to the images of the two further cameras for the above distance minimization. Take the virtual cone generated by virtual camera 1 for example. We just need to project it onto the images corresponding to virtual camera 2 and 3, because the projected virtual cones are definitely tangent to and cover the contours on the images relative to the neighboring cameras, i.e. virtual camera 4 and camera 0, as long as their translation vectors are in the directions of plane normals.

4.4. Virtual Images

To use the IBVH technique for 3D object reconstruction in this mirror image setting, we have to know the image seen by each camera in addition to the camera parameters. According to [5], we know that the real camera and its reflected virtual cameras will see the same image if we do not make the camera coordinate systems consistent. Therefore, we only need to decide which contour in the image is obj_0 viewed by the corresponding virtual camera.

To describe the relation, we firstly define the notation $CamView_a^b$ to represent the image of obj_b seen by camera a.

As shown in Figure 6, the position of obj_0 viewed by each virtual camera has the following relationship:

$$\begin{aligned} CamView_1^0 &= CamView_0^1 \\ CamView_2^0 &= CamView_0^2 \\ CamView_3^0 &= CamView_1^2 = CamView_0^4 \\ CamView_4^0 &= CamView_2^1 = CamView_0^3 \end{aligned} \quad (24)$$

5. Contours Consistence from Multiple-Views

A model reconstructed via IBVH from only 5 different views is still very rough. To refine the model, we can integrate multiple views under this setting.

Note that the above 3D reconstruction is up to an unknown scale, and the orientations and translations for the 3D reconstructed models between different views are also unknown. The alignment of the 3D reconstructed models is difficult under perspective projection, especially when a good initial guess for the alignment parameters is not available.

To simplify the refinement step under this setting, we only allow pose of one of the mirror be changed. Therefore, we fix the poses of camera 0 and virtual camera 1 (or virtual camera 2) and change the pose of the other mirror. Thus, the alignment is automatically done, and the model could be refined whenever a new view under this constraint is added.

6. Experimental Results

In this session, we show some experimental results of applying the proposed structure from reflection algorithm to reconstruct 3D object models from images containing multiple mirror reflections. The 3D reconstruction results are shown for both synthetic and real data.

6.1. Synthetic Data

In this part, we used the Stanford bunny model to generate the synthetic data, example images are shown in Figure 10. We generate five images with different mirror poses, and each image is the size of 1600x1200. Focal length is set to be 2000. As described in section 5, to simplify the consistency among multiple images, we fix the pose of the left mirror and the camera parameters across all views in generating the synthetic images.

(a) (b) (c)

Figure 10. Example views for reconstruction

For each image, we can reconstruct a rough 3D model from five different viewing angles, and some examples of the reconstruction results are shown in Figure 11.

Furthermore, we combine the five images which contains 17 (25-8) different viewing angles to reconstruct the model. The reconstruction results of four different poses are shown in Figure 12. The estimated camera poses and their spatial relationship to the object are shown in Figure 13. In Figure 13, the recovered camera centers are represented by blue points, and the ground truth is marked as red circle. Ideally, the red circle should be centered at the blue point. In Table 1, we show the reconstruction results in comparison to the ground truth. The error in the orientation estimation is the difference of rotation angle (in degree) of each rotation axis. The translation error is measured by the differences in the associated directions (in degree) and its lengths (in percentage). Because the reconstruction is up to a scale, the difference of length is expressed in percentage by dividing the length by twice the distance from the real camera to the left mirror plane.

(a) (b)

Figure 11. Examples of 3D reconstruction results from one image

As for the focal length, because the camera parameters are the same across images, we enforce this constraint by initializing the focal length as the averaged focal length of the estimates from all images and then minimizing eq.(10) . Finally, the estimated focal length is 2002.396 in this experiment.

Table 1. Accuracy of the recovered camera parameters

	Rx (°)	Ry (°)	Rz (°)	T (°)	T (%)
err avg.	0.092	0.071	0.118	0.001	0.145
err std.	0.085	0.063	0.093	0.001	0.118

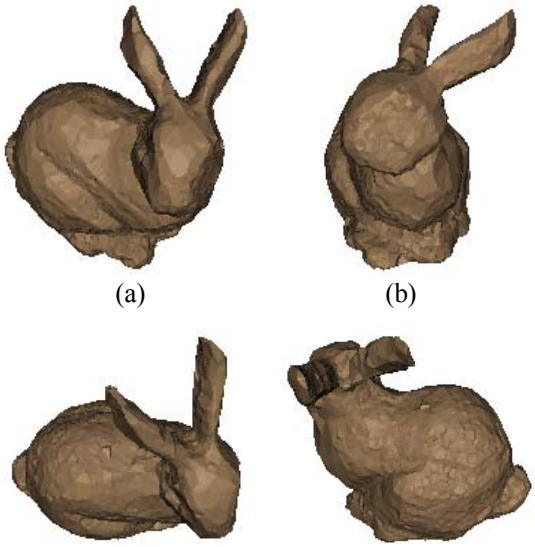

(a) (b) (c) (d)

Figure 12. Integrated reconstruction results from five images

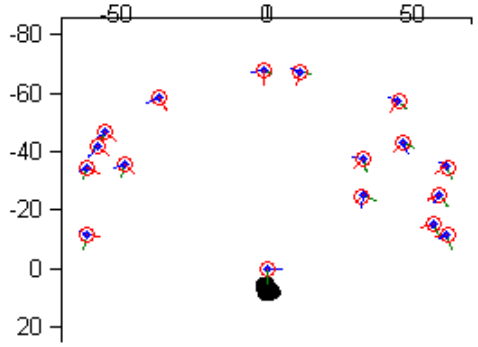

Figure 13. Estimated camera positions of the 17 viewing poses

6.2. Real Data

For the experiment on real data, we reconstructed a toy model from only one image given in Figure 1 by using the proposed structure from reflection algorithm. The results are shown in Figure 14 displayed from six different viewpoints.

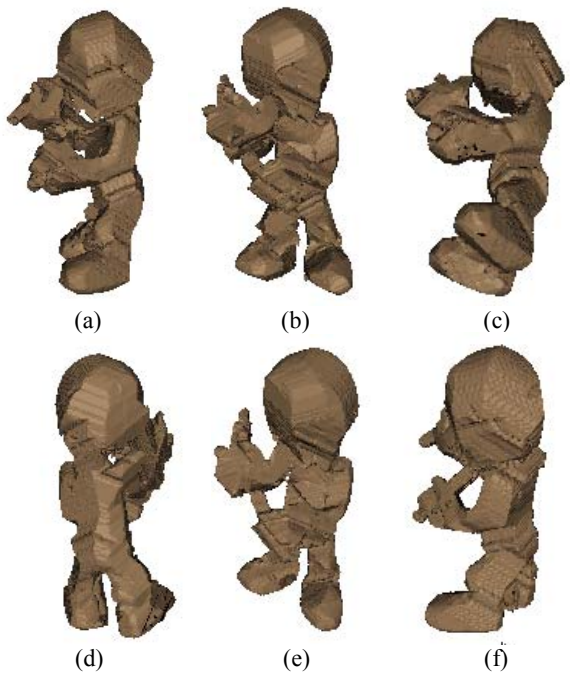

Figure 14. 3D reconstruction from a real image

6.3. Comparison

In [10], Forbes et al. proposed a closed-form solution for estimating the focal length according to the geometrical similarities. The derived closed-form solution is problematic when the angle between two mirrors is smaller than 60 degree because of the changing relationship of the epipoles and the corresponding geometrical similarities. Due to the space limitation, we cannot explain the details in this paper. Experimental results of the focal length estimation method by using their method and the proposed solution are shown in Figure 15. The experimental setup is the same as that in section 6.1.

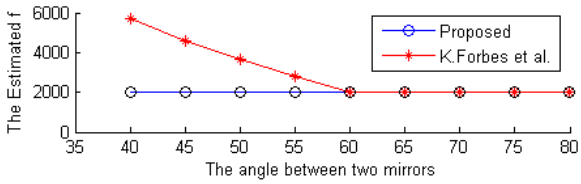

Figure 15. The comparison of focal length estimation method

7. Conclusion

In this paper, we proposed a novel metric reconstruction method from a single uncalibrated image by using two plane mirrors. Our algorithm does not make any assumption on the mirror poses. The feature correspondences needed for self-calibration can be automatically determined by finding the tangent lines between the object and its reflection. The camera intrinsic and orientations are determined by using the property of mirror reflection. The translation vectors of the corresponding virtual cameras are estimated by minimizing the distance between the object contour and the projected visual cone of a reference camera. After the real and virtual camera parameters are estimated, the 3D object model is reconstructed via the IBVH technique. Furthermore, the model can be refined by combining the 3D reconstruction from multiple mirror images. Experimental results of applying the proposed algorithm to both synthetic and real data are shown to demonstrate its performance.

Acknowledgements

This work was supported by National Science Council, Taiwan, under the grant NSC 94-2213-E-007-088.

References

[1] H. Mitsumoto, S. Tamura, K. Okazaki, N. Kajimi, and Y. Fukui, "3-D Reconstruction Using Mirror Images Based on a Plane Symmetry Recovering Method", *IEEE Trans. on Pattern Analysis Machine Intelligence*, 14(9):941-946, 1992.

[2] Z. Y .Zhang and H. T. Tsui, "3D Reconstruction from a Single View of an Object and Its Image in a Plane Mirror", *In Proc. Int. Conf. on Pattern Recognition*, 2:1174-1176, 1998.

[3] C. A. Rothwell, D. A. Forsyth, A. Zisserman, and J. L. Mundy, "Extracting Projective Structure from Single Perspective Views of 3D Point Sets", *In Proc. Int. Conf. on Computer Vision*, 573-582, 1993.

[4] W. Matusik, C. Buehler, R. Raskar, S. J. Gortler and L. McMillan, "Image-Based Visual Hulls", *In Proc. SIGGRAPH 2000*, 369-374, 2000.

[5] A. R. J. Francois, G. G. Medioni, and R. Waupotitsch, "Reconstructing Mirror Symmetric Scenes From a Single View Using 2-View Stereo Geometry", *In Proc. Int. Conf. on Pattern Recognition*, 4:12-16, 2002.

[6] D. Q. Huynh, "Affine Reconstruction from Monocular Vision in the Presence of A Symmetry Plane", *In Proc. Int. Conf. on Computer Vision*, 476-482, 1999.

[7] K. Forbes, A. Voigt and N. Bodika, "Visual Hulls from Single Uncalibrated Snapshots Using Two Planar Mirrors", *In Proc. 15th Annual Symposium of the Pattern Recognition Association of South Africa*, Nov 2004.

[8] W. N. Martin and J. K. Aggarwal, "Volumetric Descriptions of Objects from Multiple Views", *IEEE Trans. on Pattern Analysis Machine Intelligence*, 5(2):150– 158, 1983.

[9] R. Szeliski, "Rapid octree construction from image sequences", *Computer Vision, Graphics, and Image Processing. Image Understanding*, 58(1):23–32, 1993.

[10] K. Forbes, F. Nicolls, G. de Jager and A. Voigt, "Shape-from-Silhouette with Two Mirrors and an Uncalibrated Camera", *In Proc. 9th European Conference on Computer Vision*, 2006